Integrated Simulation Program for Initial Design of Bird-Inspired Ornithopter

H.-H. Yang, S.-G. Lee, E.-H. Lee, and J.-H. Han*
Korea Advanced Institute of Science and Technology, 291 Daehak-ro, Yuseong-gu, Daejeon, Republic of Korea

ABSTRACT

This study presents an integrated simulation program for the initial design of a bird-inspired ornithopter. The design and analysis of an ornithopter is a challenging task due to the complex interaction between the unsteady aerodynamic loads and wing structural deformation during the flapping flight. This study focuses on the design of a single-joint ornithopter model. The unsteady vortex lattice method (UVLM) is modified and used to predict the aerodynamic loads generated by flapping motion. The commercial software RecurDyn is used for multi-flexible-body dynamics (MFBD) analysis, and a flexible wing model is modeled using beam and shell elements. The wing kinematics of the ornithopter model is based on a planar crank-rocker. The proposed aerodynamic model is validated against the experimental results and the operation procedure of the developed ORNithopter Integrated Simulation Program (ORNISP) is introduced. As an example of the use of ORNISP, the effect of wing flexibility on ornithopter aerodynamics is analyzed.

1 INTRODUCTION

An ornithopter is an aircraft that achieves flight by flapping its wings, mimicking the flight characteristics of biological fliers. At low Reynolds numbers, the flapping motion of an ornithopter results in complex unsteady flows, which are utilized for efficient flight. Various research groups have been developing different types of ornithopters to mimic bird flight characteristics such as rapid maneuverability, camouflage, and efficient flight[1, 2, 3]. Especially, J. Gerdes *et al.*[4] developed the Robo Raven which is a servo-driven ornithopter capable of outdoor aerobatics using independently actuated and controlled wings.

However, the design and analysis of the bio-inspired flapping-wing air vehicle (FWAV) have unique challenges, primarily induced by the interaction between the unsteady aerodynamic loads and wing structural deformation during the flapping flight. Typically, the aerodynamic characteristics of FWAVs are investigated through a computational fluid-structure interaction (FSI) based on computational fluid dynamics (CFD) and computational structural dynamics (CSD) solvers[5, 6, 7]. One of the most prominent obstacles in the design process is the considerable computational time required by both CFD and CSD solvers. CFD, important for performing unsteady aerodynamic analysis, is notably time-intensive. Similarly, CSD, employed to analyze wing deformation induced by unsteady aerodynamic loads, also requires significant computation time. W. Yang *et al.*[8] developed a bird-inspired ornithopter, named DOVE, using CFD and CSD solvers, but a wing model with good lift and thrust generation was selected by comparing only three different types of flexible wing models. These extensive computational requirements of CFD and CSD often hinder the comprehensive understanding of the aerodynamic characteristics of ornithopters during the initial design stages, particularly when exploring various design parameters such as wing shape and wing kinematics.

Q. Wang *et al.*[9] proposed a computationally efficient FSI model to enable the parametric study and optimization of flapping wing twists and corresponding kinematics. The proposed model enables full FSI analysis in just a few minutes since an analytical twist model and a quasi-steady aerodynamic model are used as the structural and aerodynamic models, respectively. Similarly, R. Schwab *et al.*[10] proposed a low-order FSI model that uses a modal-analysis-based structural model and a quasi-steady aerodynamic model: blade element theory (BET). However, both FSI models have a low fidelity in unsteady aerodynamic analysis because the quasi-steady aerodynamic model, which cannot consider the nonlinearity of the wake effect, was applied to a flapping-wing model. In order to improve the fidelity, since the wake induced by flapping motion has a significant effect on unsteady aerodynamics in flapping flight, it is necessary to use an aerodynamic model that can take this into account[11, 12].

In this study, an integrated simulation program for the initial design of a bird-inspired ornithopter, named ORNithopter Integrated Simulation Program (ORNISP), is proposed. The unsteady vortex lattice method (UVLM), which can consider wake-shedding, is modified and implemented to compute the aerodynamic loads produced by the flapping motion. The multi-flexible-body dynamics (MFBD) analysis is carried out by using the commercial software RecurDyn. A flexible wing model is modeled using beam and shell elements and is converted into a modal-based flexible model. The wing kinematics of the ornithopter model is based on a planar crank-rocker

*Email address(es): jaehunghan@kaist.ac.kr

mechanism. The proposed aerodynamic model is validated against experimental results, and the operation procedure of the developed ORNISP is introduced. As an example of the use of ORNISP, the effect of wing flexibility on ornithopter aerodynamics is analyzed.

2 MATERIALS AND METHOD

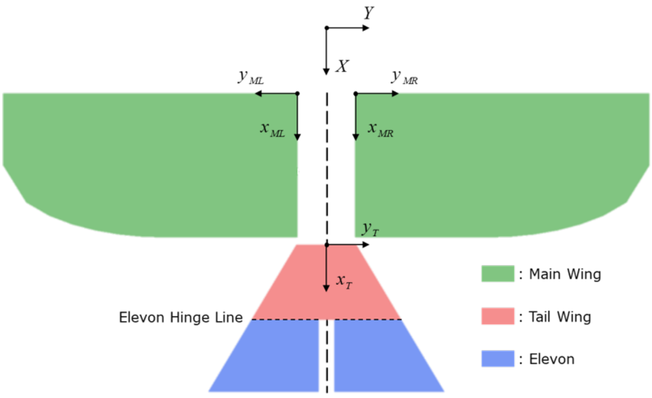

Figure 1: Schematic diagram of ornithopter model

2.1 *Ornithopter Model*

Figure 1 shows the schematic diagram of the ornithopter model. This study employs a single-joint ornithopter model in which the main wing undergoes flapping motion only about the x-axis of each body-fixed frame (x_{MR}, x_{ML}). As shown in Figure 1, the ornithopter model is composed of two main wings and one tail wing with applied elevons. Each elevon can rotate along the hinge line connected to the tail wing, and its angle can be adjusted to generate control forces for pitching or rolling moments.

2.2 *Aerodynamic Model*

This study utilizes the unsteady vortex lattice method (UVLM), which is based on potential flow theory, to compute the aerodynamic loads generated by the flapping motion of the ornithopter. In the body-fixed frame that is fixed on the wing, a velocity potential ($\mathbf{\Phi}$) can be defined. The flow around the wing is considered incompressible, inviscid, and irrotational, resulting in the continuity equation being expressed as the Laplace equation, represented as:

$$\nabla^2 \mathbf{\Phi} = \mathbf{0}. \tag{1}$$

Laplace's equation can be solved using vortex ring elements[13]. By superimposing these vortex ring elements, the complex flows around the moving wing can be simulated.

As depicted in Figure 2, the wing model has chord and span lengths of c and b, respectively, and is divided into M chord-wise and N span-wise panel elements for numerical analysis. Each panel element is assigned i and j indices,

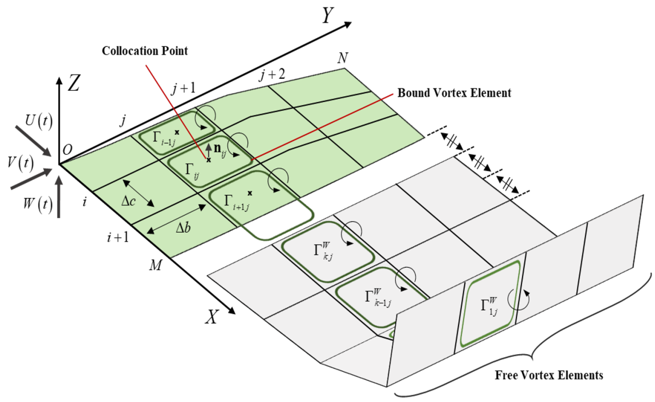

Figure 2: Schematic diagram of modified UVLM

where i denotes the chord-wise index and j denotes the span-wise index of the panel element. A uniform vorticity is assumed on each panel element and replaced with a bound vortex ring of strength Γ_{ij} located at the edge of the panel element. Here, Γ_{ij} represents the vortex strength of the bound vortex ring on the (i, j) th panel element. The middle of each panel element, where the zero normal flow boundary condition is enforced, serves as the collocation point. The normal vector of each panel element is denoted as $\mathbf{n}_{ij}$.

The wakes are simulated using free vortex ring panels of strength Γ^W_{kj} that are shed from the trailing edge of the wing. Here, Γ^W_{kj} represents the vortex strength of the free vortex ring of the k th time step and j th span-wise wake panel element. The shedding of the wake panel element begins at one-third of the distance between the trailing edge and the last free vortex ring. This shedding location is advantageous as it allows for the consideration of not only the wing motion but also the convection of the previous shed vortices[14, 15].

To calculate the pressure difference (Δp_K), a vorticity vector ($\boldsymbol{\gamma}_K$) is employed, and the unsteady Bernoulli equation is utilized as follows:

$$\Delta p_K(t) = \rho \Bigg[\{ (U(t) + u_W, V(t) + v_W, W(t) + w_W)_K \times \boldsymbol{\gamma}_K \} \cdot \mathbf{n}_K + \frac{1}{\Delta t} \left(\sum_{K=1}^{m} \Gamma_K(t) - \sum_{K=1}^{m} \Gamma_K(t - \Delta t) \right) \Bigg] \tag{2}$$

where ρ is the flow density, and $(U(t), V(t), W(t))_K$ represents the kinematic velocity due to the wing's motion, while $(u_W, v_W, w_W)_K$ represents the induced velocity resulting from the wake panels. Additionally, Δt is the time step size of the simulation, and m is equal to $M \times N$. The aerodynamic loads are determined by integrating all the pressure differences along the surface of the wing.

This study introduces a novel numerical scheme, named the pseudo leading-edge vortex (PLEV) model shown in Figure 3, to account for the effects of flow separation and

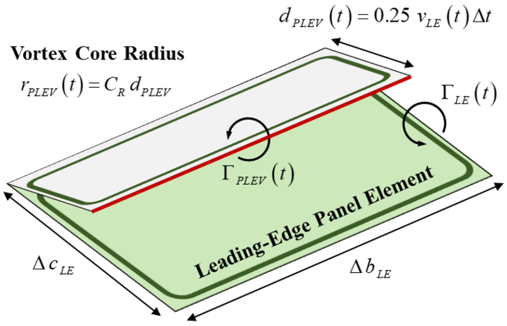

Figure 3: Schematic diagram of PLEV model

leading-edge vortex during flapping flight. The PLEV model creates a PLEV ring panel from each leading-edge panel of the wing. In this case, the trailing PLEV line is created behind the leading-edge by a distance of d_{PLEV}. The strength of the PLEV (Γ_{PLEV}) is affected by the strength of the leading-edge panel (Γ_{LE}) and its local induced velocity (v_{LE}). Moreover, the vortex core radius of the PLEV (r_{PLEV}) is equal to the product of d_{PLEV} and core radius coefficient (C_R).

2.3 *Multi-Flexible-Body Dynamics Model*

In the ornithopter model, the main wing can be modeled as a rigid wing to simplify the analysis by ignoring the deformation of the wing. However, in order to more accurately analyze the aerodynamic characteristics of the ornithopter, the wing should be modeled as a flexible wing, which requires a multi-flexible-body dynamics (MFBD) analysis for the entire model.

In this study, the commercial software RecurDyn is employed as the solver for the MFBD analysis. At first, a finite element (FE) model of a flexible wing is modeled using beam and shell elements. The beam elements represent the wing frame structures such as spars and ribs in the main wing. The shell elements represent the wing sheet structure to which aerodynamic loads are enforced. This FE flexible wing model is further converted into a modal-based flexible wing by modal analysis since the FE model requires considerable computational time for analysis.

In order to consider the interaction between the aerodynamic model and the structural model, a straightforward coupling method termed the nearest-neighbor interpolation is introduced. In this method, a node in the aerodynamic mesh of the wing (Figure 2) is coupled with the nearest node in the structural mesh (Figure 4 (B)), resulting in both nodes having the same deformation. The aerodynamic force acting on an aerodynamic node is applied at the nearest structural node from the collocation point. The validity and effectiveness of this simple coupling method have been proved in the research conducted by A. T. Nguyen and J.-H. Han[16].

The FSI, which uses the modified UVLM as an analysis method for unsteady aerodynamics and a modal-based flexible model as a structural model, can provide highly efficient and reliable analysis results although its accuracy is lower than FSI using CFD and CSD solvers.

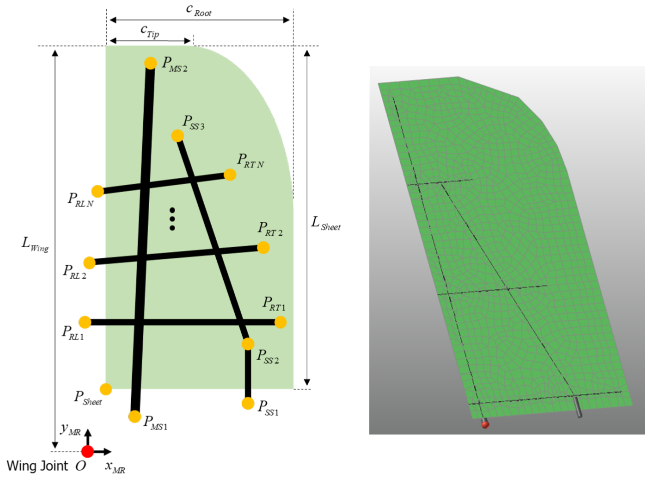

Figure 4: (A) Schematic diagram of the main wing, (B) Flexible wing model with structural mesh

2.4 *Wing Kinematics*

The ornithopter model used in this study employs a flapping mechanism based on the planar crank-rocker mechanism, which is one of the widely used mechanisms in ornithopters. The schematic diagram of the planar crank-rocker mechanism is illustrated in Figure 5, where the angle of the fixed link is denoted as ϕ_0, the length of the fixed link is denoted as L_0, the length of the crank is denoted as L_1, the length of the coupler is denoted as L_2, the length of the rocker is denoted as L_3, the transmission angle is denoted as μ, and the flapping angle is denoted as θ.

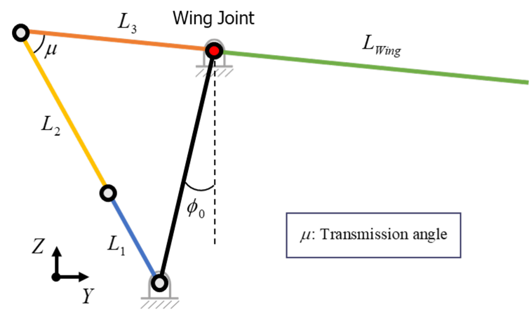

Figure 5: Schematic diagram of planar crank-rocker

The length of each link is obtained through parameter optimization. The optimization problem is solved to search for design parameters with an average transmission angle close to 90deg when given the minimum and maximum transmission angles, upside flapping angle, and downside flapping angle.

In this study, the minimum and maximum transmission angles are set to 45deg and 135deg, respectively. Also, the upside and downside flapping angles are set to 45deg and 15deg, respectively. The optimization is performed using the genetic algorithm, one of the global optimization algorithms. The genetic algorithm generates a random population and keeps the elite child for the next generation. It reaches the global minimum by utilizing crossover and mutation algorithms. In this optimization problem, the population size is 5000 which is 1000 times the number of inputs (ϕ_0, L_0, L_1, L_2, L_3); elite-child and crossover rates are, respectively, 4% and 70% (mutation rate = 26%). The final outputs of the optimization are the angle of the fixed link and each length of the links, and the values are as follows: $\phi_0 = 12deg$, $L_0 = 37.6mm$, $L_1 = 10.0mm$, $L_2 = 33.5mm$, $L_3 = 20.0mm$).

3 Results and Discussion

3.1 *Validation for Aerodynamic Model*

In order to validate the proposed aerodynamic model (modified UVLM with the PLEV model), wind tunnel tests were conducted on two different wing models: a rigid wing model and a flexible wing model. A rectangular plate wing was selected as the wing shape for the test. Both wings have 130mm of chord and 250mm of wing length: the aspect ratio is almost two. The rigid wing model consists of a balsa wood wing sheet with a thickness of 1 mm, and main- and sub-spars made of carbon fiber reinforced plastic (CFRP) pipes with outer and inner diameters of 4 mm and 3 mm, respectively. The flexible wing model has a wing sheet made of polyester with a thickness of 0.012 mm and a main spar made of a CFRP pipe with the same dimensions as the rigid wing model, but no sub-spar. The rib of the flexible wing model is made of a CFRP rod with a diameter of 0.8 mm.

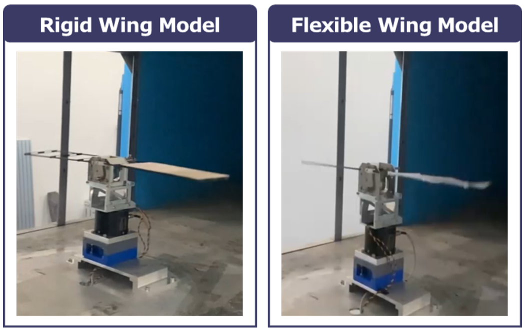

Figure 6: Test model mounted in the KAIST subsonic wind tunnel

Wind tunnel tests were performed at a flow speed of 5.5 m/s and at different geometric angles of attack ranging from 0 to 25 degrees, with a flapping frequency of 2.5 Hz. The lift and thrust were measured using a 3-axis load cell (MC15-3C-50), while the flapping motion was actuated by a DC motor (GM35-2932E) and measured using a laser displacement sensor (IL-600). The test models are mounted in the KAIST subsonic wind tunnel as shown in Figure 6.

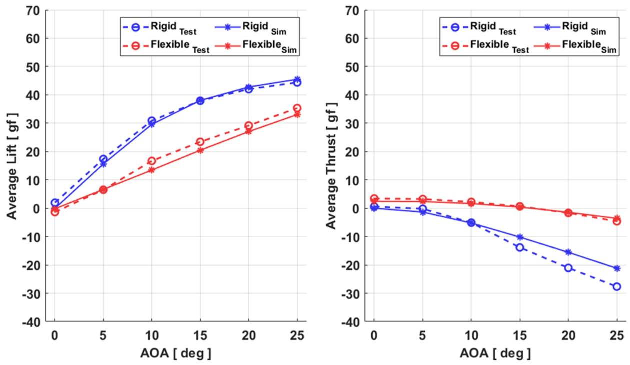

Figure 7: Cycle-averaged lift and thrust of test models

Figure 7 shows the cycle-averaged lift and thrust of the test models. The validation results of the proposed aerodynamic model using the modified UVLM showed a lift error of less than 1.7% and a thrust error of less than 13.5% for the rigid wing model. For the flexible wing model, the model showed a lift error of less than 5.1% and a thrust error of less than 16.9%. While there is room for improvement in terms of thrust estimation, it can be concluded that the modified UVLM provides a sufficiently accurate estimation for flapping aerodynamics in forward flight. The proposed approach takes only 42 seconds for the three cycles of the flexible wing model. Although the validation model is a single wing, the computation time within one minute means that the proposed FSI model is quite efficient in terms of computational time and can guarantee the fidelity of unsteady aerodynamic analysis for the flapping-wing model.

3.2 *ORNithopter Integrated Simulation Program*

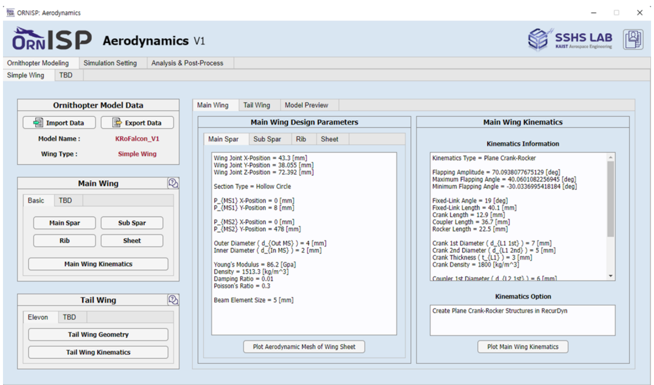

Figure 8: Main screen of ORNISP

ORNithopter Integrated Simulation Program (ORNISP) is an aimed program for aerodynamic analysis in designing ornithopters. It was developed as a MATLAB App, which

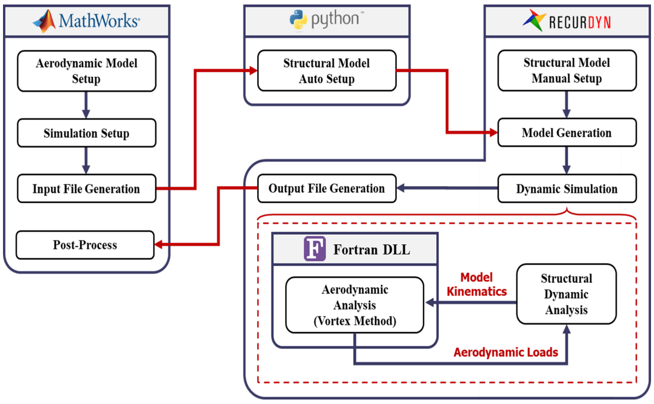

Figure 9: Configuration and flow diagram of ORNISP

consists of MATLAB, Python, and RecurDyn, and its main screen is shown in Figure 8. The program has a dedicated data format (*.omdat) for managing model data, and all information, such as the design parameters, kinematics, and UVLM simulation parameters of the ornithopter model, is classified and managed. Figure 9 shows the configuration and flow diagram of ORNISP. The MATLAB GUI allows adjusting the parameters of the wing flap mechanism model to be analyzed. Additionally, input files that have geometric information about the wing configuration are generated using MATLAB to create wing structures in RecurDyn. In this case, automatic model creation of the ornithopter simulation model using a Python script is possible.

The modified UVLM with the PLEV model is compiled as Fortran DLL and used in RecurDyn, enabling fluid-structure coupled analysis. After the analysis is finished, the exported CSV file can be used to perform the aerodynamic force computation and wake visualization. With ORNISP, it is possible to perform aerodynamic analysis for designing ornithopters without the extensive computational requirements of CFD and CSD solvers. The integration of the modified UVLM and PLEV models with RecurDyn, along with the flexibility of the wing model, allows for a comprehensive understanding of the aerodynamic characteristics of ornithopters during the initial design stages. Overall, ORNISP provides a user-friendly interface and automated workflow for the aerodynamic analysis of ornithopter designs.

3.3 *Effect of Wing Flexibility on Aerodynamics*

Unsteady aerodynamic simulations were performed for the two ornithopter models whose configurations are shown in Figure 1: rigid main wing and flexible main wing. Both wings have 200mm of mean chord and 490mm of wing length, and the overall geometric shape and dimensions are shown in Figure 10. The flight condition of the ornithopter model was determined based on the reduced frequency of Festo's Smart Bird[3]. Hence, in this study, the flapping frequency of 3.5 Hz, the forward flight speed of 6 m/s, and the geometric angle of attack of 5 deg were selected.

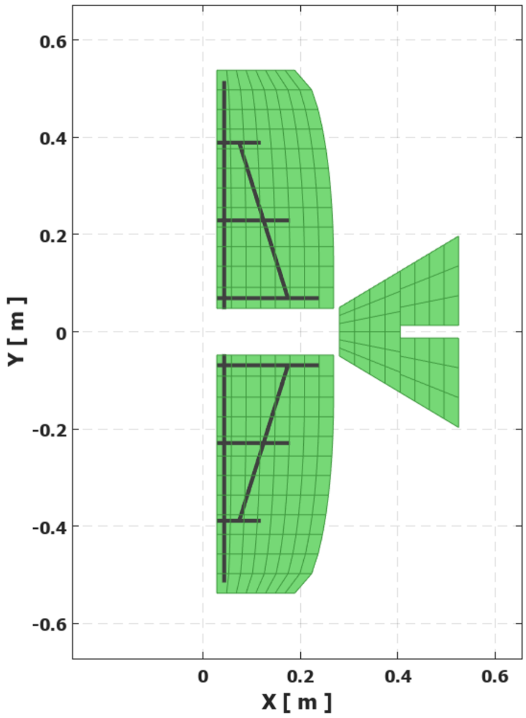

Figure 10: Geometric shape and dimensions of the simulation model

Figure 11 illustrates the comparison between the rigid wing and flexible wing models in terms of the lift coefficient (C_L). It can be observed that the rigid wing model produces a lift value similar to that of the flexible wing model. However, as shown in Figure 12, the rigid wing exhibits a negative mean value of thrust coefficient (C_T) under the given flight conditions, indicating its inability to achieve forward flight. In contrast, the flexible wing model demonstrates zero thrust under the given flight conditions, indicating that it is in a trim state of forward flight and capable of maintaining stable flight.

These results emphasize the importance of considering wing flexibility during the initial design stage of a bird-inspired ornithopter. The integration of flexible wing models, as demonstrated in ORNISP, allows for a more accurate assessment of the ornithopter's aerodynamic performance. By enabling the exploration of various wing designs and their effects on aerodynamics, ORNISP can provide valuable insights for optimizing the design of ornithopters with enhanced flight capabilities.

4 CONCLUSION

In this study, an integrated simulation program, named ORNithopter Integrated Simulation Program (ORNISP), has been proposed for the initial design of a bird-inspired ornithopter. To address the computational time limitations of

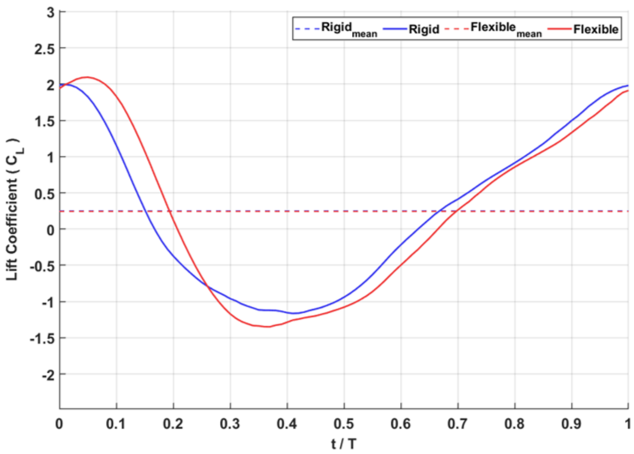

Figure 11: Time history of lift coefficient during one cycle

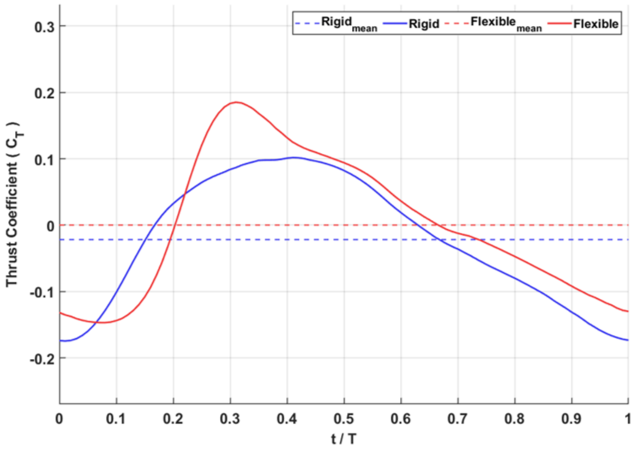

Figure 12: Time history of thrust coefficient during one cycle

CFD and CSD solvers, the UVLM was modified and implemented to efficiently compute the aerodynamic loads generated by the flapping motion. MFBD analysis was conducted using the commercial software RecurDyn. A flexible wing model, represented by beam and shell elements, was modeled and converted into a modal-based flexible model. The wing kinematics of the ornithopter model was based on the widely used planar crank-rocker mechanism. The proposed aerodynamic model was validated against experimental results, demonstrating its reliable accuracy (cycle-averaged lift error of less than 5.1%, thrust error of less than 16.9%) for the flexible wing model. The configuration of ORNISP was introduced. The effect of wing flexibility on ornithopter aerodynamics was analyzed. It was observed that considering wing flexibility is crucial, as demonstrated by the comparison between rigid and flexible wing models. The flexible wing model exhibited stable flight under the given forward flight condition, whereas the rigid wing model showed unfavorable flight characteristics (negative cycle-averaged thrust).

In conclusion, this research presents ORNISP as a promising integrated simulation program for the efficient and effective initial design of bird-inspired ornithopters. ORNISP offers a user-friendly interface and automated workflow, eliminating the extensive computational requirements associated with CFD and CSD solvers. Future work will focus on expanding the capabilities of ORNISP to include more complex ornithopter models and wing kinematics, as well as broadening its application range to other bio-inspired micro air vehicles.

ACKNOWLEDGEMENTS

This research was supported by Unmanned Vehicles Core Technology Research and Development Program through the National Research Foundation of Korea (NRF) and Unmanned Vehicle Advanced Research Center (UVARC) funded by the Ministry of Science and ICT, the Republic of Korea (2020M3C1C1A01083415).

REFERENCES

[1] A. Chen, B. Song, Z. Wang, D. Xue, and K. Liu. A novel actuation strategy for an agile bioinspired fwav performing a morphing-coupled wingbeat pattern. *IEEE Transactions on Robotics*, 39(1):452–469, 2023.

[2] G. A. Folkertsma, W. Straatman, N. Nijenhuis, C. H. Venner, and S. Stramigioli. Robird: A robotic bird of prey. *IEEE Robotics Automation Magazine*, 24(3):22–29, 2017.

[3] W. Send, M. Fischer, K. Jebens, R. Mugrauer, A. Nagarathinam, and F. Scharstein. Artificial hinged-wing bird with active torsion and partially linear kinematics. In *28th ICAS Congress*, Brisbane, Australia, 2012.

[4] J. Gerdes, A. Holness, A. Perez-Rosado, L. Roberts, A. Greisinger, E. Barnett, J. Kempny, D. Lingam, C.-H. Yeh, H. A. Bruck, and S. K. Gupta. Robo raven: A flapping-wing air vehicle with highly compliant and independently controlled wings. *Soft Robotics*, 1(4):275–288, 2014.

[5] J. Tang, S. Chimakurthi, R. Palacios, C. E. S. Cesnik, and W. Shyy. Computational fluid-structure interaction of a deformable flapping wing for micro air vehicle applications. In *46th AIAA Aerospace Sciences Meeting and Exhibit*, Reno, Nevada, 2008.

[6] T. Nakata and H. Liu. A fluid-structure interaction model of insect flight with flexible wings. *Journal of Computational Physics*, 231(4):1822–1847, 2012.

[7] V. Joshi, R. K. Jaiman, and C. Ollivier-Gooch. A variational flexible multibody formulation for partitioned fluid-structure interaction: Application to bat-inspired drones and unmanned air-vehicles. *Computers*

and Mathematics with Applications, 80(12):2707–2737, 2020.

[8] W. Yang, L. Wang, and B. Song. Dove: A biomimetic flapping-wing micro air vehicle. *International Journal of Micro Air Vehicles*, 10(1):70–84, 2018.

[9] Q. Wang, J. F. L. Goosen, and F. van Keulen. An efficient fluid-structure interaction model for optimizing twistable flapping wings. *Journal of Fluids and Structures*, 73:82–99, 2017.

[10] R. Schwab, E. Johnson, and M. Jankauski. A novel fluid–structure interaction framework for flapping, flexible wings. *Journal of Vibration and Acoustics*, 141(6):061002, 2019.

[11] J. Wu and M. Sun. The influence of the wake of a flapping wing on the production of aerodynamic forces. *Acta Mech Sinica*, 21:411–418, 2005.

[12] D.-K. Kim, J.-S. Lee, and J.-H. Han. Improved aerodynamic model for efficient analysis of flapping-wing flight. *AIAA Journal*, 49(4):868–872, 2011.

[13] J. Katz and A. Plotkin. *Low-Speed Aerodynamics*. Cambridge University Press, Cambridge, UK, 2001.

[14] S. A. Ansari, R. Żbikowski, and K. Knowles. Nonlinear unsteady aerodynamic model for insect-like flapping wings in the hover. part 2: Implementation and validation. *Proc. Inst. Mech. Eng. Part G: Journal of Aerospace Engineering*, 220(3):169–186, 2006.

[15] H.-H. Yang, S.-G. Lee, R. Addo-Akoto, and J.-H. Han. Parameter optimization of foldable flapping-wing mechanism for maximum lift. *Journal of Mechanisms and Robotics*, 16(3):031002, 2024.

[16] A. T. Nguyen and J.-H. Han. Wing flexibility effects on the flight performance of an insect-like flapping-wing micro-air vehicle. *Aerospace Science and Technology*, 79:468–481, 2018.